ORIGINAL PAPER

Performance Evaluation of Moment-Resisting Steel Frame Buildings Under Seismic and Blast-Induced Vibrations

Muhammed Zain Kangda[1] · Sachin Bakre[2]

Abstract

Purpose The paper is an attempt to evaluate the efficiency of passive control techniques such as base isolation system (e.g. Lead/Rubber Bearing) and fluid viscous dampers subjected to earthquake ground motions and underground blast-induced vibrations. Two moment-resisting steel frame buildings are analyzed to evaluate the structural responses under dynamic excitations. The effect of vertical irregularity on the performance of passive control techniques in mitigating the responses of the building is also studied.

Methods Non-linear dynamic analysis has been conducted on regular and irregular steel structures. The study investigates the effect of isolation period on the structural responses. The isolators are designed based on the design procedures developed by various researchers. The technical specifications of fluid viscous dampers have been selected from M/s Taylor Devices, USA.

Results The structural responses and energy dissipated by these control techniques is evaluated and a comparative study is also carried out amongst control techniques under blast and seismic excitations.

Conclusions Both the selected passive control techniques have proved to be very effective in reducing the structural responses and forces induced in the building owing to ground-induced vibration.

Keywords Blast-induced vibration · Base isolation · Energy dissipation · Earthquake · Fluid viscous damper · Passive techniques

Introduction

Researchers in the field of structural control have developed numerous structural control methodologies in the area of earthquake engineering. These methods are now being implemented into practice and safeguard structures against natural calamities like earthquakes and in high rise buildings subjected to large wind forces. In the recent years, research directed towards the protection of various civil engineering structures subjected to different blast-induced shocks has gained extensive attention. The reasons associated with this research are mainly due to increased mining activities, inhuman acts like terrorism, accidental explosions, etc., causing tragic destructions to human life and structural assets. In India, the codes of practice to calculate blast loads are classified based on the locations of their occurrence, namely, underground blasts [1] and above-ground blasts [2]. In the present study, the effects of underground blast-induced vibrations on protective structures have been evaluated. The regulations and guidelines laid by the other international codes of practice [3–5] also help structural engineers and researchers to calculate the intensity of blast loads within their permissible limits.

Various researchers have conducted experimental tests to establish empirical formulae to calculate blast parameters required to estimate a blast load. Kumar et al. in [6] summarized attenuation relationships proposed by various researchers to calculate important blast load parameters in the form of peak particle velocity (PPV) for different soil sites. The empirical formulae to calculate the PPV based on the effect of amplification of explosion waves due to soil stratifications were proposed by Rigas and Sebos in [7]. Wu et al. in [8] conducted blast tests to examine the difference in blast wave characteristics on soil surface, at soil-rock interface and also inside the rock mass for granite rock deposit in Sweden.

✉ Muhammed Zain Kangda
  zainkangda@gmail.com

1 Applied Mechanics Department, Visvesvaraya National Institute of Technology, Nagpur, India

2 Department of Applied Mechanics, Visvesvaraya National Institute of Technology, Nagpur, India

Later, Wu and Hao in [9] validated the recorded data with the help of a numerical model. The study also derived relationships for peak particle acceleration, peak particle velocity and the principal frequency over ground surface and on free field medium.

In addition to the above-mentioned studies, vibration control techniques to mitigate this erratic and complex phenomenon also need serious attention. In the field of blast-resistant structures, the application of structural control techniques is limited to [10–12] and hence reviewed in the present study. Soong and Dargush in [13] have broadly classified the modern structural protective techniques into three main groups, namely, base isolation (elastomeric bearings, lead/rubber bearings and sliding friction pendulum), passive energy dissipation devices (metallic dampers, viscous dampers, tuned mass dampers, etc.) and semi-active and active control devices (active mass dampers, active bracing systems, etc.) to safeguard present and existing structures from transient environmental events. In the field of earthquake engineering, these techniques have been extensively studied by [14–18]. The base isolation technique has been well researched by Constantinou and Tadjbakhsh [19], Kelly et al. [20], Johnson et al. [21], Jangid and Kelly [22] and others in the field of earthquake engineering. The effectiveness of different energy-absorbing devices in mitigating the earthquake effects on structures located in seismically active regions was demonstrated by Housner et al. in [23]. The displacement-based design for buildings equipped with passive control techniques, such as viscous, visco-elastic and friction dampers, has been formulated by Lin et al. in [24]. The optimal locations of these supplemental devices in mitigating the structural responses subjected to seismic excitations have also been evaluated by Kokil and Shrikhande in [25], Singh and Moreschi in [26], Dargush and Sant in [27] and Park et al. in [28].

Another important aspect of the study includes the analysis of these techniques employed in structures plagued with vertical irregularity in the form of geometric irregularity. Di Sarno et al. in [29] conducted non-linear seismic analysis on an irregular hospital building employed with a base-isolated system using a finite element model. Cancellara and Angelis in [30] studied the effectiveness of different base isolation techniques installed in reinforced concrete buildings subjected to earthquake loading with irregularities in plan. Goel in [31], applied non-linear viscous dampers to asymmetric systems in mitigating structural seismic responses.

Yet another objective of the study also includes the evaluation of energy dissipated by the selected protective devices which is a useful measure in evaluating the performance of the buildings when subjected to seismic and blast-induced vibrations.

Blast and Seismic Excitations

Based on the previous studies by Hinman in [32] and Carvalho and Battista in [33], the blast-induced ground vibration in terms of ground acceleration, $\ddot{x}_{g}(t)$ is modeled as an exponential decaying function indicated by Eq. 1:

$$\ddot{x}_{g}(t) = -\frac{1}{t_{d}}v\,e^{\frac{-t}{t_{d}}} \tag{1}$$

In the above equation, v (m/s) is the peak particle velocity (PPV) obtained from the empirical equation proposed by Kumar et al. [34] using digitization software for various rock characteristics. Equation 2 is derived from the curve-fitting technique to obtain the PPV so that the proposed equation can be compared properly with the available field data cases. The present study evaluates the blast-induced ground acceleration data for granite rock deposit. The material properties of granite to be substituted in Eq. 2 to obtain PPV are Young's modulus, $E = 73.9$ GPa; average mass density, $\gamma_{d} = 26.50$ kN/m^3; and uniaxial compressive strength, $f_{c} = 70$ MPa. These material constants are selected from the study by Kumar et al. [34].

$$v = \frac{f_{c}^{0.642}\mathrm{SD}^{-1.463}}{\gamma_{D}} \tag{2}$$

Moreover, the scaled distance, SD (m/kg$^{1/2}$) is determined as the ratio of distance from charge point, R (m) to the square root of charge mass (Q). The present study is carried out for a constant value of $R = 100$ m. The charge weight values vary from 10 tons to 75 tons. A plot of the blast-induced ground acceleration is shown in Fig. 1 so that the arrival time, t_{d}, is evaluated using the expression $t_{d} = R/c$, where c is the wave-propagation velocity (m/s) in soil obtained as the square root ratio of E and γ_{d} of granite rock as discussed above. The plots for blast-induced vibrations are developed from the mathematical expressions suggested by Carvalho and Battista in [33]. In addition to the blast-induced vibrations, the structures are also subjected to four real seismic excitations as shown in Fig. 2.

The earthquakes include some of the most commonly cited seismic records, namely, Imperial Valley earthquake (magnitude 6.6, 1979), Northridge Earthquake (magnitude 6.7, 1994) and San Fernando Earthquake (magnitude 6.6, 1971) for non-linear dynamic analysis of the selected buildings. The responses of the buildings have also been evaluated for the New Zealand Earthquake (magnitude 6.2, 2011).

Analytical Building Model

In the present study, the moment resisting steel buildings as studied by Whittle et al. [35], to obtain effective damper placement techniques has been selected to evaluate

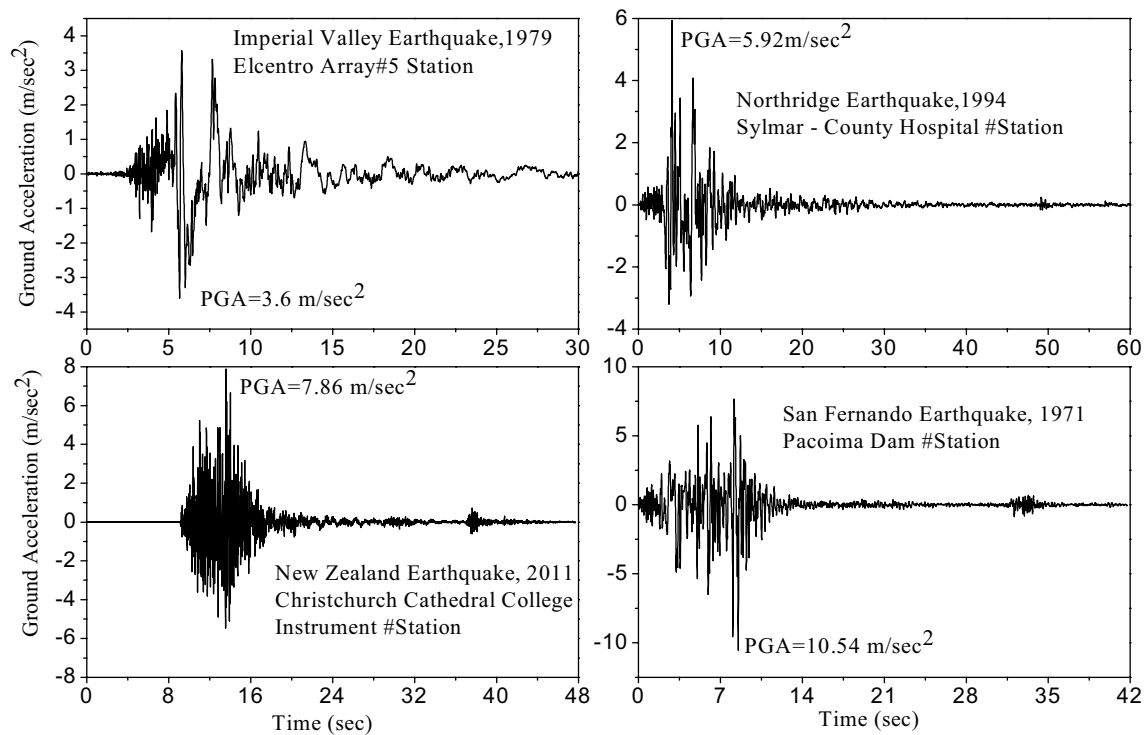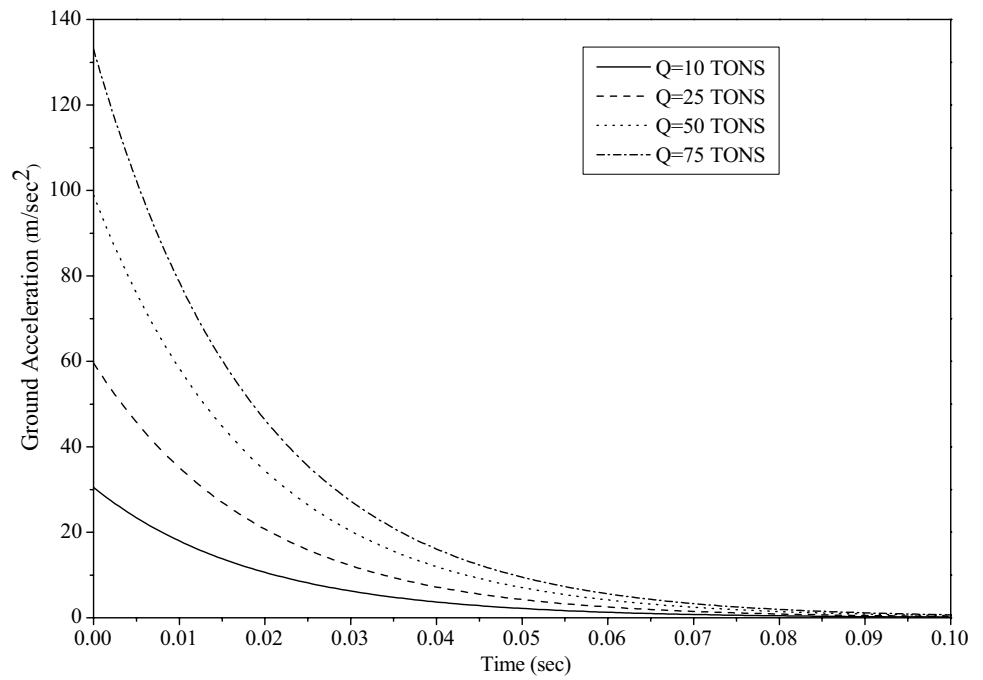**Fig. 1** Blast-induced ground acceleration time histories

Fig. 2 Selected earthquake records

its performance under blast and seismic ground motions with the help of structural analysis and design tool using SAP2000 software [35]. The building configuration along with its prescribed properties based on the Eurocode [36] is

as shown in Fig. 3. Figure 3b reveals that the base length (L_1) is 3 times the top storey length (L_2) thereby resulting in vertical geometric irregularity as prescribed by various international standards [37–39] for building design. Non-linear

dynamic analysis is performed using Newmark's step-by-step non-linear direct integration method assuming linear variation of acceleration ($\gamma = 0.5$ and $\beta = 0.25$) to study the structural response over the time interval, dt. The material non-linearity is also incorporated in the study with non-linear properties assigned to viscous dampers and lead/rubber bearing systems. The analysis is carried out with the help of structural analysis and design tool, SAP2000 software. The maximum time interval dt for earthquake motions plotted in Fig. 2 is 0.005 s. Blast is a short duration phenomenon and occurs only for a few milliseconds and hence to capture the performance for such short duration loading, time step parameter for blast loading as discussed in "**Blast and seismic excitations**" is d$t = 0.0005$ s. The maximum structural responses obtained from the above explained procedure are tabulated in Tables 1 and 2 to compare the performance of fixed base regular and irregular buildings respectively.

It is observed that the presence of irregularity increases the damage indices such as top storey peak displacement, acceleration and internal forces in the buildings. Further, passive control techniques such as LRB and fluid viscous dampers (FVD) as indicated in Fig. 4 are employed to both regular and irregular buildings to study the effectiveness of control techniques under blast and seismic excitations.

Base-Isolated System—Regular and Irregular Buildings

In the field of earthquake resistant structures, innovation in the form of base isolation systems have resulted in reduced
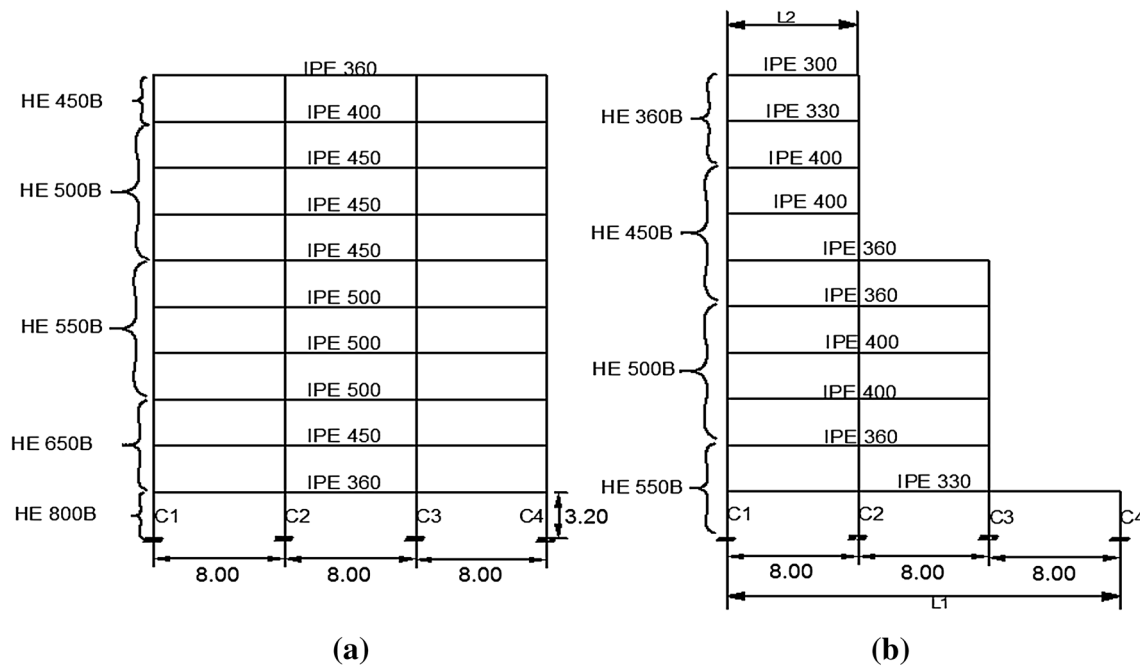

Fig. 3 Building properties **a** front elevation of regular building and **b** irregular building elevation (all units in meters)

Table 1 Peak responses of fixed-base regular building under dynamic loadings

Ground excitation	Peak top storey drift (mm)	Peak top storey displacement (mm)	Peak top storey absolute acceleration (m/s^2)	Peak maximum bending moment (kNm)	Peak maximum base shear (kN)
Blast 1	33.35	271.0	6.18	1535.70	387.14
Blast 2	65.18	530.0	12.10	3001.12	756.77
Blast 3	108.23	880.0	20.07	4984.27	1256.51
Blast 4	145.60	1180.0	27.0	6705.22	1690.35
Imperial Valley	44.73	520.0	7.27	3935.11	756.10
Northridge	58.96	682.60	9.10	4405.51	820.34
New Zealand	13.81	128.97	3.63	1218.88	280.60
San Fernando	41.94	296.0	10.26	2336.10	479.10

Table 2 Peak responses of fixed-base irregular building under dynamic loadings

| Ground excitation	Peak top storey drift (mm)	Peak top storey displacement (mm)	Peak top storey absolute acceleration (m/s^2)	Peak maximum bending moment (kNm)	Peak maximum base shear (kN)
Blast 1	59.74	368.10	7.70	834.25	327.42
Blast 2	116.76	719.50	15.05	1630.76	640.03
Blast 3	193.87	1194.64	25.0	2707.65	1062.69
Blast 4	260.81	1607.12	33.62	3642.54	1426.60
Imperial Valley	113.15	961.66	10.37	2220.54	333.17
Northridge	137.64	1021.43	13.22	2169.24	341.78
New Zealand	30.0	209.26	4.80	607.73	140.57
San Fernando	83.41	404.03	15.24	1130.63	310.93
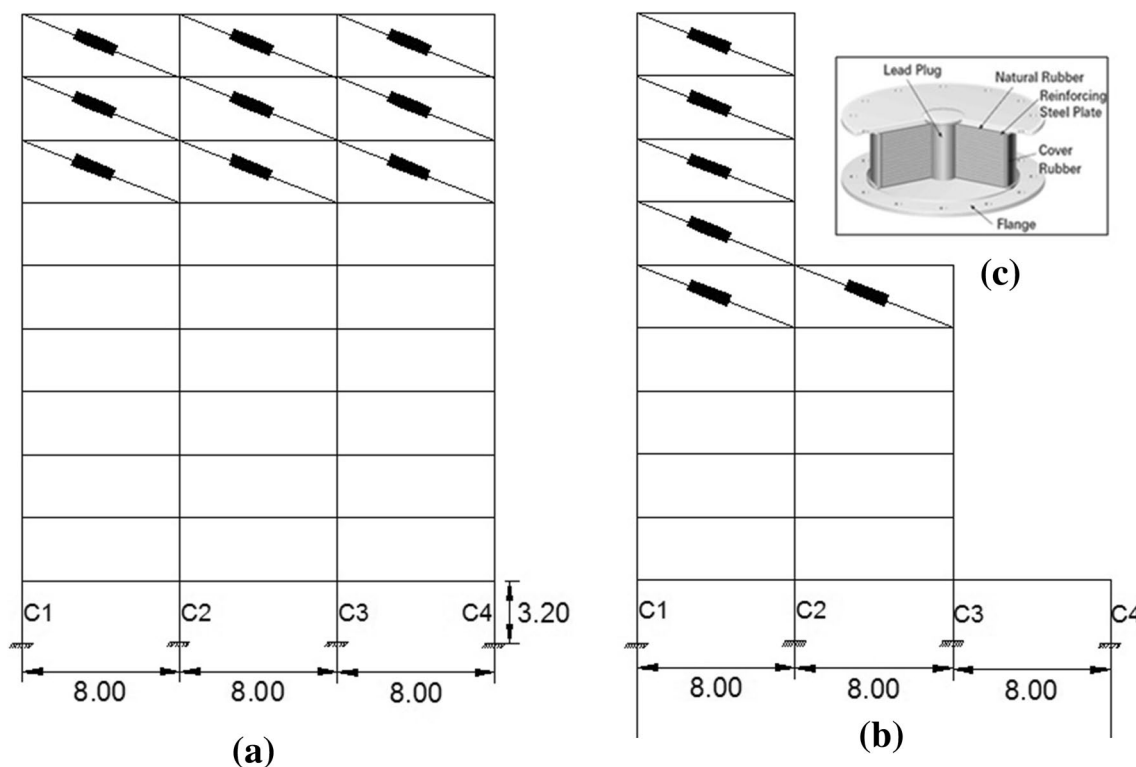
Fig. 4 Building installed with FVDs **a** regular building and **b** irregular building, **c** prototype of base isolation system (LRB)

displacements and forces incurred to the buildings and other civil engineering structures. The main objective of base isolation is to provide an additional means of energy dissipation, thereby reducing the transmitted acceleration to the superstructure. In addition, the decoupling makes the building flexible, thereby improving its response to earthquakes. In this study, the concept of base isolation is applied to both regular and irregular structures in order to evaluate building performance under both blast and seismic excitations. The guidelines proposed by [16] are followed to design the lead/rubber bearing systems. In the current research

work, the effect of isolation period (T_b) on the building performance is also studied. The period of isolation is taken as $T_b = 1.5 T_s$, $T_b = 2.0 T_s$ and $T_b = 3.0 T_s$ where T_s is the structure period. The other assumed isolation parameters include 15% isolation damping (η), yield stress of lead core, $F_y = 10342$ kN/m^2 and the shear modulus of rubber, $G = 414$ kN/m^2.

The design spectral acceleration at 1 s period (S_{D1}) is an essential parameter for determining the design displacement of isolators and can be estimated for the building conditions as studied by [35] and is equal to 0.45 g. A summary of

isolation properties obtained from the seismic design handbook calculated from the weight of the structure is illustrated in Table 3. The output results display that an LRB system, which has an isolation period three times the structure period is best suited in mitigating the structural responses incurred in buildings constructed with a fixed-base system. The study evaluates the reduction in storey drift values obtained at different floor levels of a ten-storey regular building and a ten-storey irregular building. The results are plotted in Figs. 5 and 6 for regular and irregular base-isolated buildings, respectively. It is observed that the best-suited isolation technique ($T_b = 3\ T_s$) yields top storey drift reductions in the range 70–85% under blast and 60–88% under seismic excitations for regular buildings. In case of irregular buildings, the reductions are in the range 77–88% under blast and 62–83% under earthquake loading. Thus it can be observed that the isolation technique is very effective in reducing the top storey drift of regular and irregular fixed-base buildings.

The study also compares the performance of regular and irregular base-isolated buildings subjected to blast and earthquake excitations in mitigating the top storey displacement and absolute acceleration indices and the results are shown in Fig. 7. It is observed that the selected isolation systems are very effective in mitigating the structural responses under blast and seismic excitations. The top storey acceleration values are reduced by approximately 90% for all cases of blast-induced vibrations, but under seismic conditions the displacement and acceleration reductions range in between 60–84 and 74–83%, respectively.

The performance of the selected base-isolated systems in mitigating the structural responses of regular and irregular buildings under blast and seismic excitations is also compared in Tables 4 and 5, respectively. It is evident from the study that the base isolation technique draws maximum reductions of 50–60% in base shear and 60–70% in maximum bending moment forces under blast loading, whereas the maximum base shear and bending moment responses are reduced to 50–90 and 70–90% under seismic excitations for regular buildings. In case of irregular buildings, the design of selected lead/rubber isolators harvests an improved performance in blast and seismic loading conditions and the results are tabulated in Table 5. Thus an isolation period equivalent to three times the

structural period results in optimal structural reductions for a regular and an irregular fixed-base building.

In addition to this, the study evaluates the force displacement behaviour of the isolated system under Column, C_2 and is plotted in Figs. 8 and 9 for regular and irregular buildings, respectively. It is observed that an isolation period of $T_b = 3\ T_s$ results in maximum bearing displacement with least value of shear force resulting in maximum hysteretic energy dissipated as can be seen in the case of blast-induced loading for regular and irregular buildings in Figs. 10 and 11. The hysteretic energy is evaluated using the energy-conversion equation concept proposed by Uang and Bertero in [40] and given by Eq. 3, where E_i is the absolute input energy, E_k is the absolute kinetic energy; E_s is the elastic recoverable strain energy; the non-negative damping energy is represented by E_ξ.

$$E_i = E_k + E_\xi + E_s + E_h \tag{3}$$

$$E_h = \int_0^t F_b \dot{x}\, dt - \frac{(F_b)^2}{2k_b} \tag{4}$$

$$E_d = \frac{100E_h}{E_i} \tag{5}$$

The irrecoverable hysteretic energy (E_h) is determined using Eq. 4 where F_b is the restoring force developed in the isolating device and k_b is the stiffness of the isolating device. The percentage energy dissipated (E_d) by the vibration control technique is also obtained by Eq. 5. It is also observed that in case of seismic excitations, an increase in the isolation period reduces the energy dissipated along with input energy. Next, fluid viscous dampers are investigated as these are considered an alternative to the base isolation technique [41].

Fluid Viscous Damper—Regular and Irregular Buildings

The base isolation technique reviewed above to mitigate the structural responses can also be replaced with control

Table 3 Designed isolator properties for regular and irregular buildings ($T_b = 3T_s$)

| Isolator properties	Regular building				Irregular building			
	Column 1 (C1)	Column 2 (C2)	Column 3 (C3)	Column 4 (C4)	Column 1 (C1)	Column 2 (C2)	Column 3 (C3)	Column 4 (C4)
Effective stiffness (K_{eff})	215.60	414.31	414.31	215.60	165.95	262.36	116.52	16.50
Post-yield stiffness (K_d)	164.80	316.69	316.69	164.80	126.85	200.54	89.07	12.61
Yield force (Q)	32.36	62.19	62.19	32.36	28.05	44.35	19.70	2.79
Post-yield stiffness ratio (α)	0.10	0.10	0.10	0.10	0.10	0.10	0.10	0.10
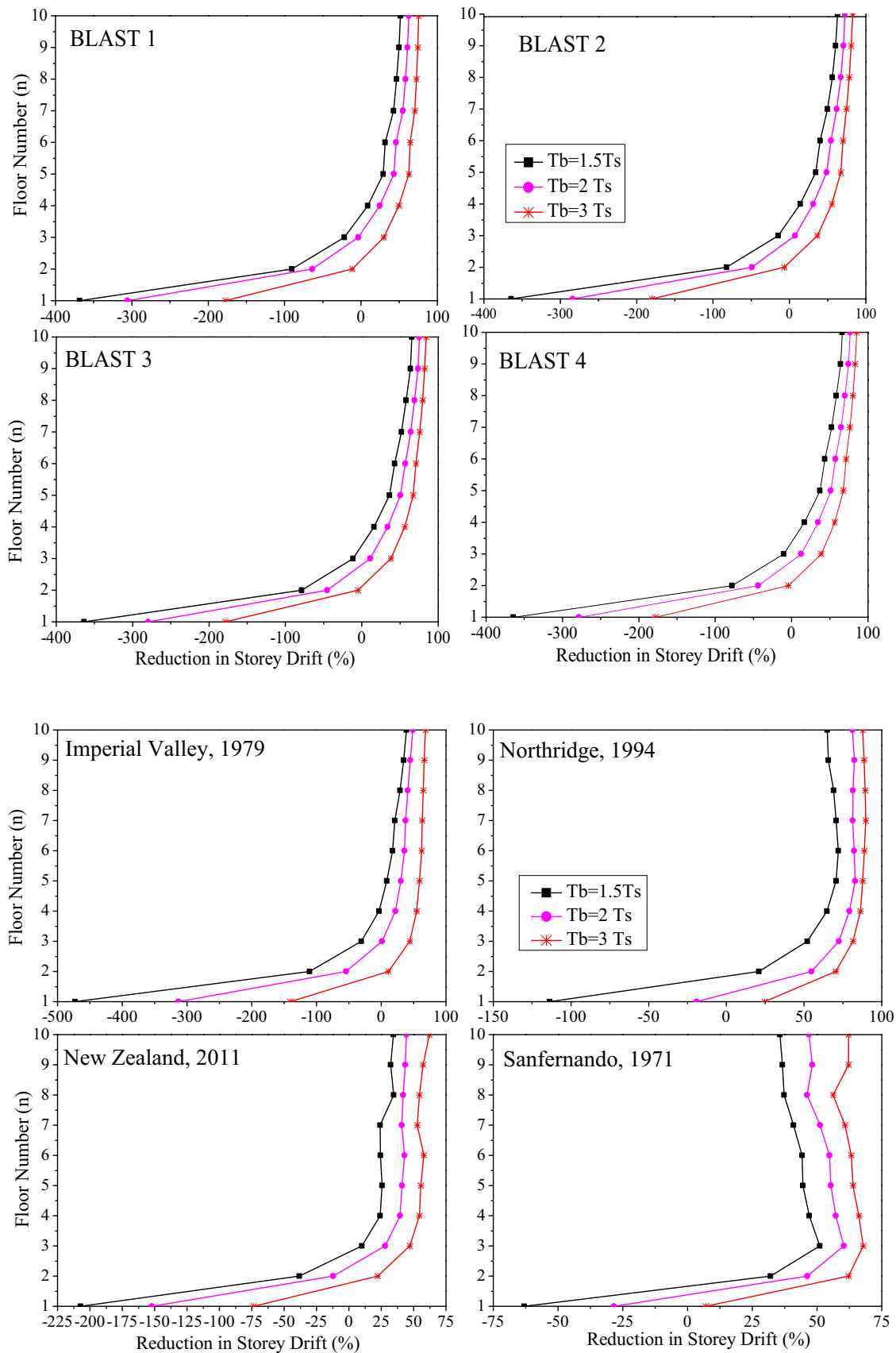
Fig. 5 Reduction in storey drift (%) in base-isolated regular buildings under dynamic excitations
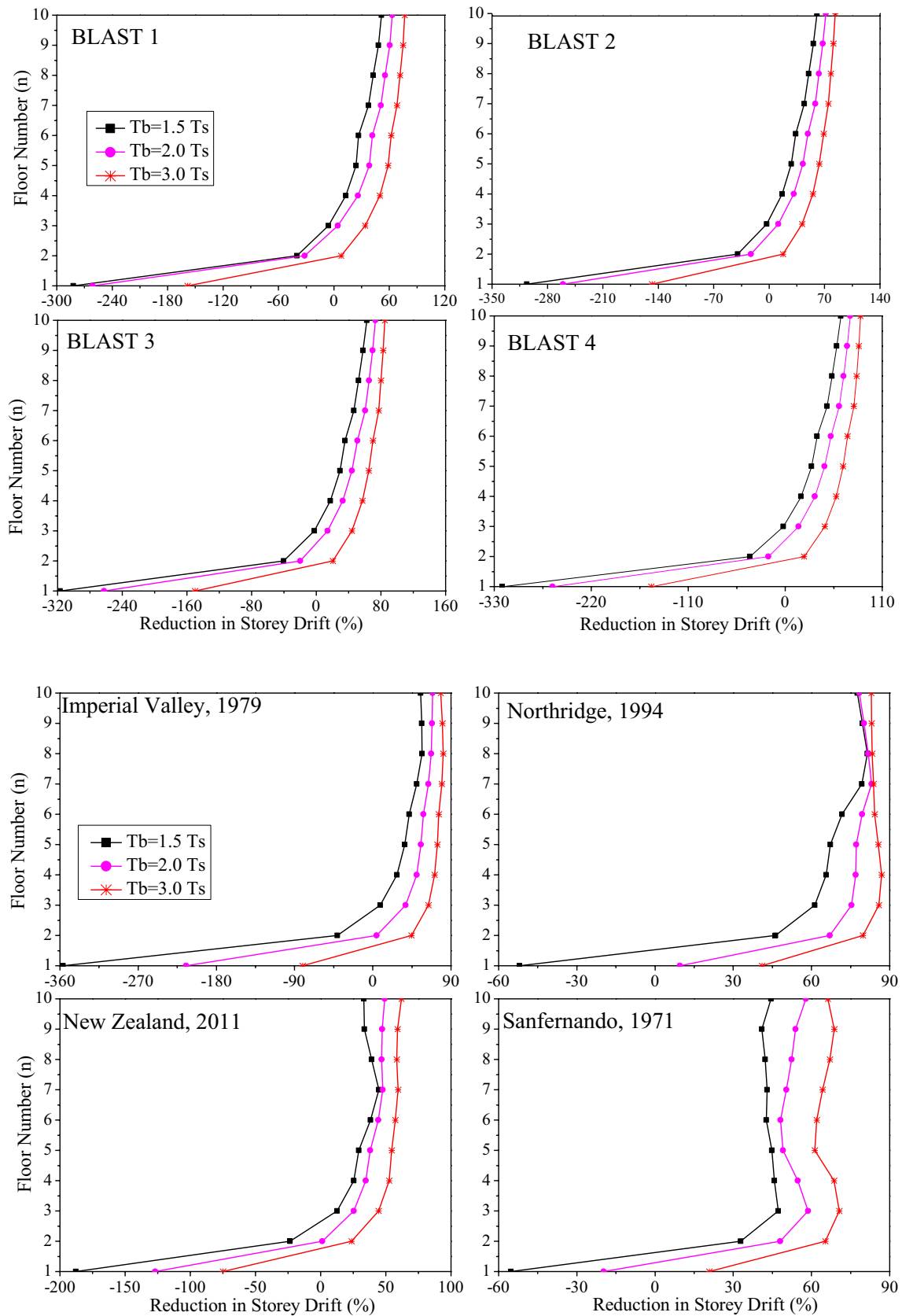
Fig. 6 Reduction in storey drift (%) under dynamic excitations in base-isolated irregular buildings
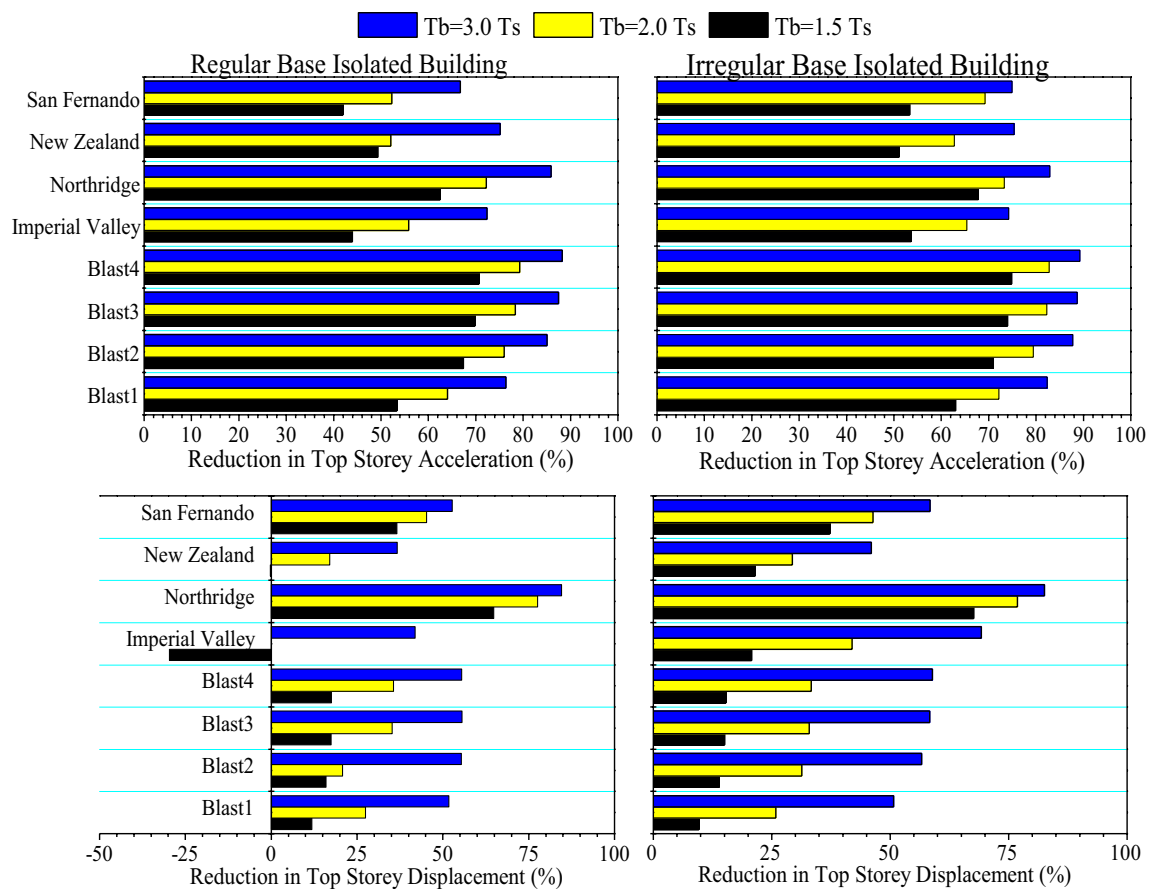
Fig. 7 Performance of base-isolated steel buildings under dynamic excitations

Table 4 Performance of base-isolated regular building under dynamic excitations

Ground excitation	$T_b = 1.5\,T_s$		$T_b = 2.0\,T_s$		$T_b = 3.0\,T_s$	
	Reduced maximum base shear (%)	Reduced maximum bending moment (%)	Reduced maximum base shear (%)	Reduced maximum bending moment (%)	Reduced maximum base shear (%)	Reduced maximum bending moment (%)
Blast 1	43.40	54.34	48.55	58.49	61.56	69.0
Blast 2	31.35	44.64	39.90	51.53	56.25	64.72
Blast 3	25.91	40.23	35.87	48.26	53.51	62.50
Blast 4	23.68	38.45	34.21	46.92	52.37	61.58
Imperial Valley	− 22.19	24.88	16.73	48.79	49.70	69.07
Northridge	60.69	76.57	80.11	88.15	89.62	93.82
New Zealand	68.81	77.03	78.24	83.98	84.01	88.22
San Fernando	84.17	89.10	86.76	91.32	90.77	93.94

devices in the form of dampers which diminish the high vibration amplitude developed in structures subjected to dynamic loading. These devices protect the structure by minimizing the energy to be dissipated by the structure, thus reducing the structural damage. The dampers are further classified based on the external source of energy required to instigate them in operation, namely, passive dampers (no external energy source required), active dampers (continuous energy source required) and semi-active dampers (less energy source required). Many researchers have studied fluid

Table 5 Performance of base-isolated irregular building under dynamic excitations

Ground excitation	$T_b = 1.5\,T_s$		$T_b = 2.0\,T_s$		$T_b = 3.0\,T_s$	
	Reduced maximum base shear (%)	Reduced maximum bending moment (%)	Reduced maximum base shear (%)	Reduced maximum bending moment (%)	Reduced maximum base shear (%)	Reduced maximum bending moment (%)
Blast 1	58.49	47.87	60.57	50.49	67.26	58.90
Blast 2	48.27	35.06	51.73	39.38	62.38	52.76
Blast 3	43.72	29.27	47.94	34.59	60.12	49.92
Blast 4	41.82	26.92	46.43	32.68	59.18	48.72
Imperial Valley	− 85.74	10.83	− 30.52	37.31	25.36	64.16
Northridge	59.68	79.66	74.37	87.08	84.19	92.03
New Zealand	70.06	77.78	76.53	82.62	82.35	86.94
San Fernando	85.35	87.39	88.36	89.76	93.13	96.95

viscous dampers (FVD) as an alternative to base isolation systems as both the control schemes exhibit passive energy dissipation technique to control the structural responses. The selected damper technique works on the principle of movement of fluid through the orifices and is similar to the action of a shock absorber in an automobile.

The FVD is characterized by a resistance force, F. It depends upon the relative velocity of the movement, fluid viscosity and the orifice size of the piston. Equation 6 shows the relation between damping force developed and the relative velocity between the ends of dampers:

$$F = C_d\,\dot{u}^\alpha \tag{6}$$

where F is the damper force, C_d is a damping constant, $\dot{u}$ is the relative velocity between the two ends of a damper and α is the exponent ranging between 0 and 1. The damper with $\alpha = 1$ is known as a linear viscous damper in which force is directly proportional to relative velocity. The damper with $\alpha > 1$ has not been often used in practical applications. The damper with $\alpha < 1$ is called a non-linear viscous damper, which is effective in minimizing high velocity shocks. Figure 12 shows the force–velocity relationship for the following types of FVDs as studied by Ras and Boumechra in [42]. Fluid viscous dampers exhibit visco-elastic behaviour which can be predicted by the Kelvin and Maxwell model for linear and non-linear dampers. In the case of a Kelvin model, a spring and a viscous damper are attached parallel to each other, whereas in the case of a Maxwell model, the spring is in series with the viscous damper. The Maxwell model is mostly used to predict the behavior of FVD. SAP 2000 adopts the Maxwell model to simulate the behavior of a damper. Figure 13 depicts the details of the two above-mentioned models. The model is described by Eq. 7. In the given equation, $u(t) = u_o \cdot \sin{(wt)}$. P is the damper output force, λ is the relaxation time, C_d is the damping constant at zero frequency and u is the displacement of the piston head with respect to the damper housing. The

relaxation time (λ) is given by Eq. 8, where, K_d is the storage stiffness of the damper at infinite frequency.

$$P(t) + \lambda\,\frac{dP(t)}{dt} = C_d\,\frac{du(t)}{dt} \tag{7}$$

$$\lambda = \frac{C_d}{k_d} \tag{8}$$

The present study analyzes the above-mentioned regular and irregular structures equipped with fluid viscous dampers under blast and seismic loading. As shown in Fig. 4, nine dampers are selected and placed at the top three storeys of a fixed-base regular building, whereas for an irregular building, six dampers are selected to improve the structural performance under blast and seismic excitations. The damper properties, tabulated in Table 6, are selected from M/s Taylor Devices, USA, as studied by Narkhede and Sinha in [43]. Figures 14 and 16 prove that Damper B-1 is the best device for regular buildings from the selected six dampers under blast and earthquake loading due to its reasonably high damping coefficient and low damper exponent. It achieves reductions of 63.78 and 40.46% in top storey drift and top storey absolute acceleration values under Blast 1 loading. But under seismic conditions, reductions of 50.80 and 53.33% have been achieved for Imperial Valley Earthquake and San Fernando Earthquake for drift and acceleration indices, respectively.

Among the Type-A dampers, Damper A-3 shows maximum reductions in damage parameters due to low damper exponent and appreciable damping coefficient. In the case of an irregular building, fluid viscous dampers further improve the structural performance in the form of drifts, top storey displacements and absolute accelerations by an additional 10–20% and are evident from Figs. 15 and 16 for different cases of dynamic loading. The performance
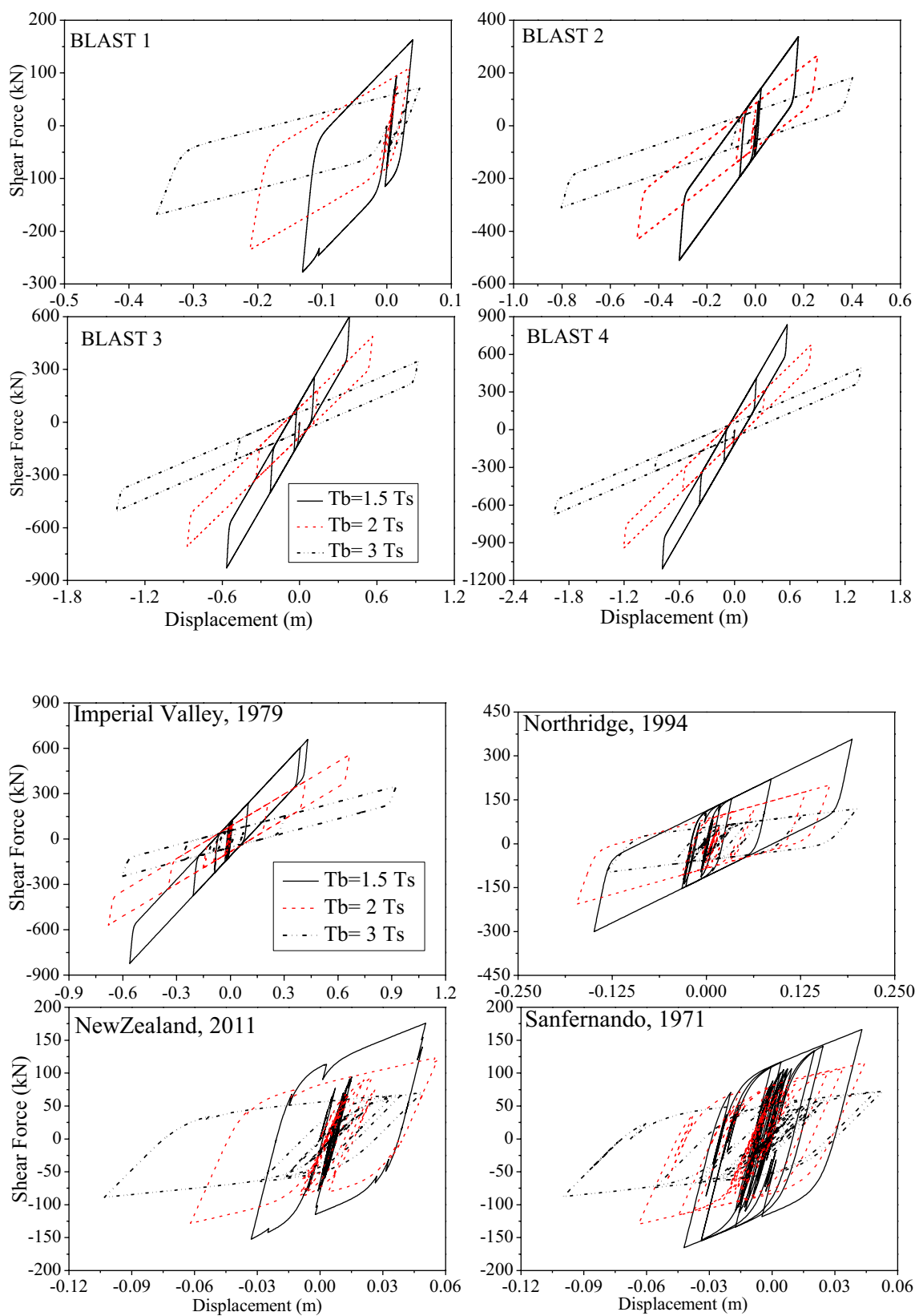
Fig. 8 Force displacement behavior of lead/rubber isolators under selected ground excitations (regular building)
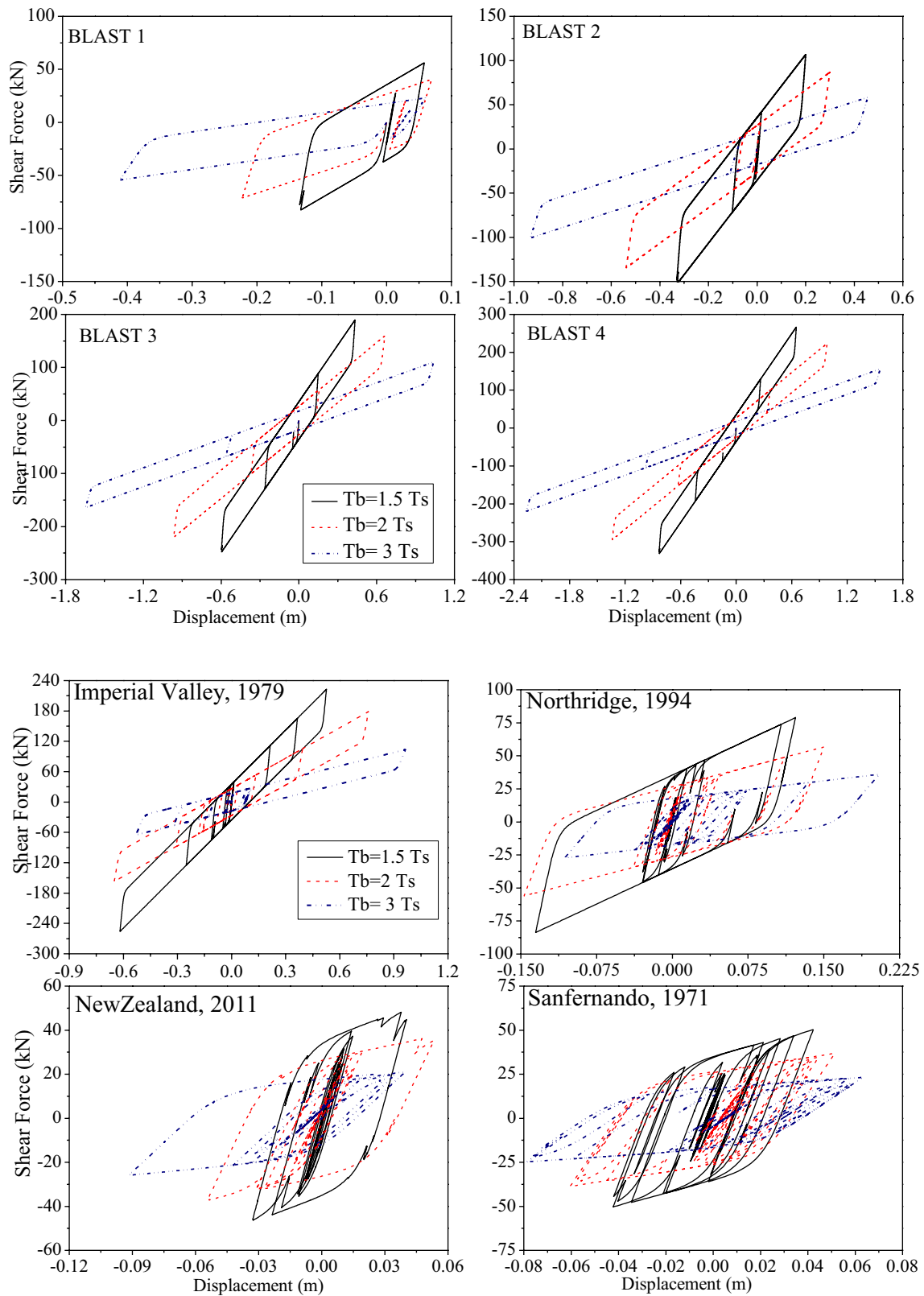
Fig. 9 Force displacement behavior of lead/rubber isolators under selected ground excitations (irregular building)
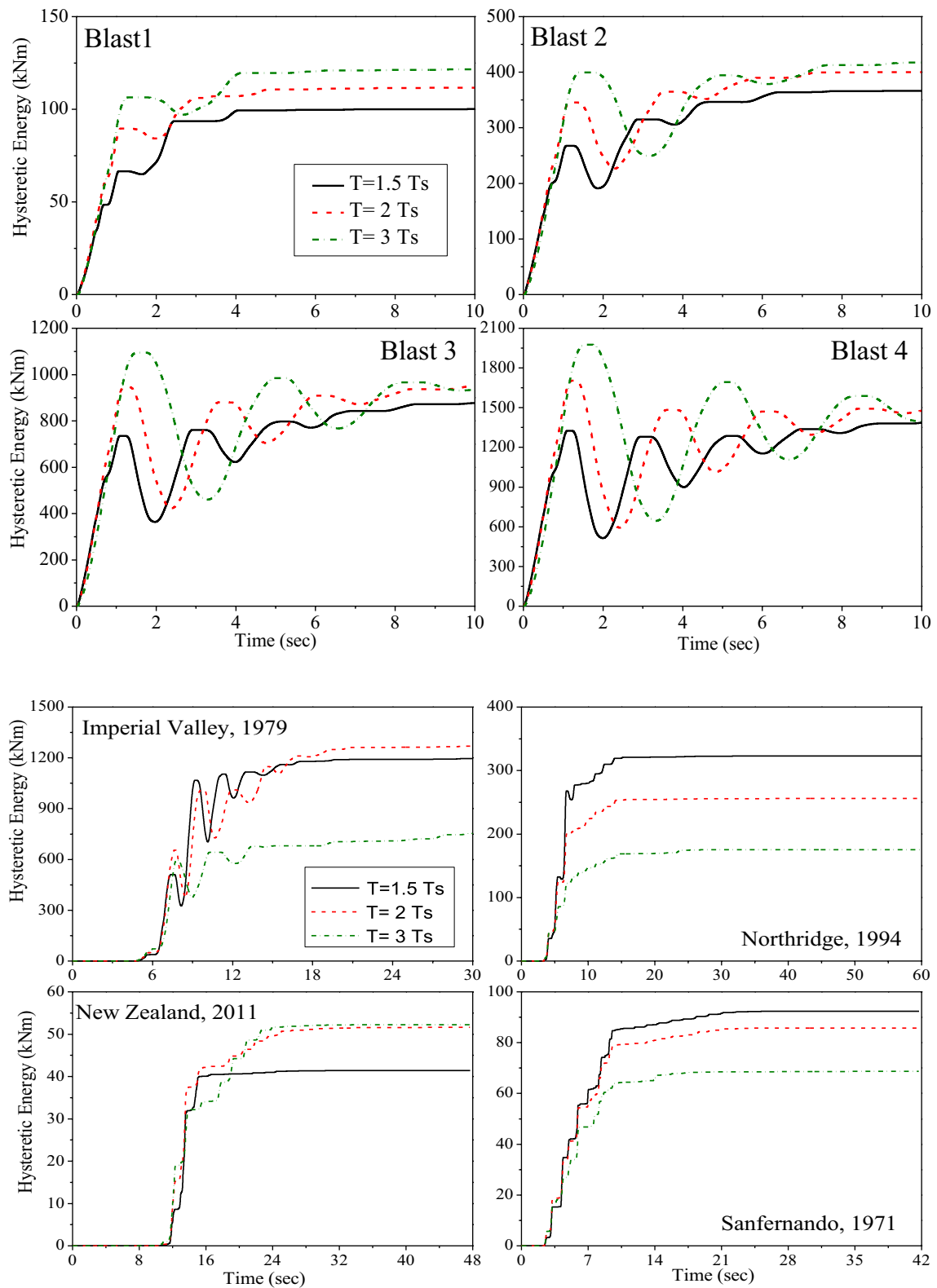
Fig. 10 Energy dissipated by base isolation systems in mitigating structural responses under selected excitations (regular building)
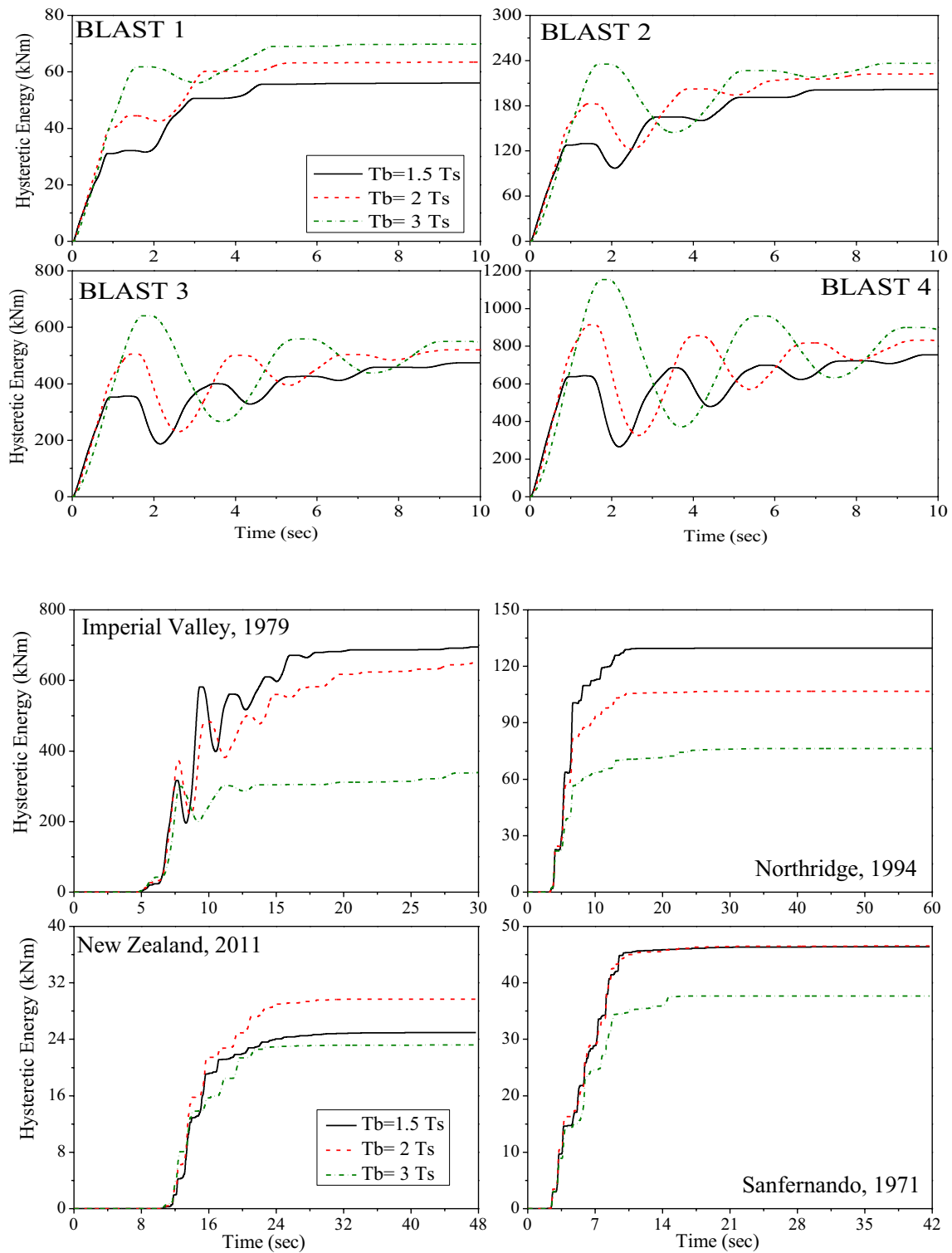
Fig. 11 Energy dissipated by base isolation systems in mitigating structural responses under selected excitations (irregular building)

of regular and irregular buildings installed with FVDs under blast and seismic excitations indicates that the regular buildings installed with FVDs achieved reductions

of 30–64 and 20–40% in drift and acceleration values, respectively, for blast-induced vibrations. Under seismic excitations reductions of 40–84 and 20–60% are achieved
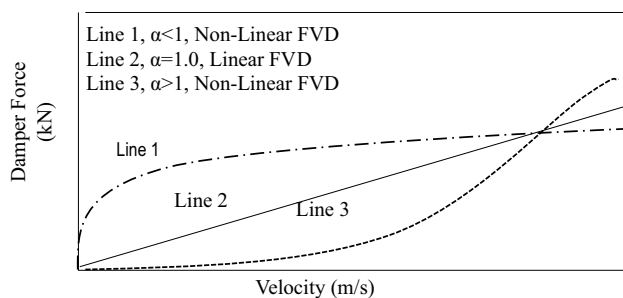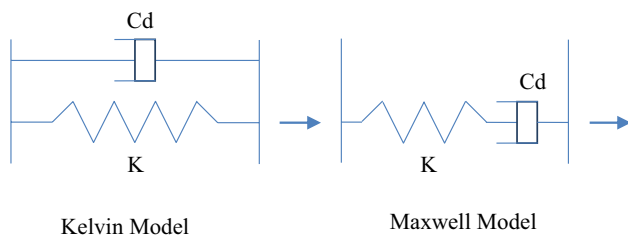
Fig. 12 Force vs. velocity relation of damper

Fig. 13 Kelvin and Maxwell model (Ras and Baumechra [31])

Table 6 Fluid viscous damper specifications, M/s Taylor Devices, USA [30]

Sr. no.	Reference	Coefficient of damper c_α (kNs/m)	Damper exponent (α)	Remarks
Damper 1 (A-1)	67DP-18921-01	420	0.8	Type A
Damper 2 (A-2)	RT50DH100	330	0.51	Type A
Damper 3 (A-3)	RT50DH200	315	0.46	Type A
Damper 4 (B-1)	67DP-18922-01	330	0.36	Type B
Damper 5 (B-2)	RT50DH100	280	0.39	Type B
Damper 6 (B-3)	RT150DH50	280	0.5	Type B

in drift and acceleration indices. For irregular buildings, the reductions obtained are 40–74 and 40–56% in drift and acceleration values, respectively, under blast loading. Reductions in drift and acceleration indices are found to be in the range 60–95 and 40–73%, respectively, under earthquake ground motions.

The comparative study of the selected buildings based on the ability to reduce member forces reveals that the installed FVDs perform better under seismic excitations as compared to blast-induced excitation since marginal reductions are obtained in shear and bending moment forces of column, C2, and the results are compiled in Tables 7, 8, 9, 10. It is

also observed that compared to other dampers, Damper B-1 proves to be the best in obtaining the maximum reduction in storey drift values at each floor level under dynamic loadings. As stated above, Damper B-1 and A-3 lead to maximum reductions in the structural damage indices and hence, its force displacement behavior is also studied. It is observed from Figs. 17 and 18 that Damper B-1 undergoes maximum axial force along with appreciable deformations resulting in maximum energy dissipated for all cases of selected ground vibrations and plotted in Fig. 19 and 20. Further it is observed that the performance of FVDs installed in regular systems shows better energy dissipation and force deformation behavior as compared to FVDs installed in irregular buildings.

The force deformation curves also summarize that though A-3 damper results in maximum displacement with appreciable axial force, the number of force deformation loops developed also governs the energy dissipation ability of a particular system. The percentage of energy dissipated by the control techniques is also compared and tabulated in Tables 11 and 12 as obtained from Eq. 5. It is observed that Damper B-1 leads to maximum energy dissipation capacity among the selected dampers, whereas LRB ($T_b = 3\ T_s$) has proven to be very effective for all the cases concerned with dynamic excitations and building geometries thus resulting in maximum vibration control. It can be stated that the input energy reduces significantly with increase in isolation period for seismic cases and hence the energy dissipation capacity increases though the hysteretic energy dissipated is less as observed in Figs. 10 and 11 for seismic cases.

Thus, the present study compares the structural performance of regular and irregular buildings equipped with lead/rubber bearings and fluid viscous dampers. The selected number of dampers results in structural performances equitable with the isolation systems. The energy dissipation capacity of both the selected passive techniques is also investigated and compared based on their inherent properties on energy conservation formulations proposed by researchers.

Summary and Conclusions

In this study, the passive control techniques, such as base isolation system (e.g., LRB) and fluid viscous dampers (FVDs) have been employed on a ten-storey regular building and a ten-storey irregular building subjected to underground blast and seismic excitations. The blast is modeled as an exponential decaying function in terms of ground acceleration, whereas the selected seismic excitations are obtained from the COSMOS strong motion database. The LRB isolators are designed in such a manner so that the
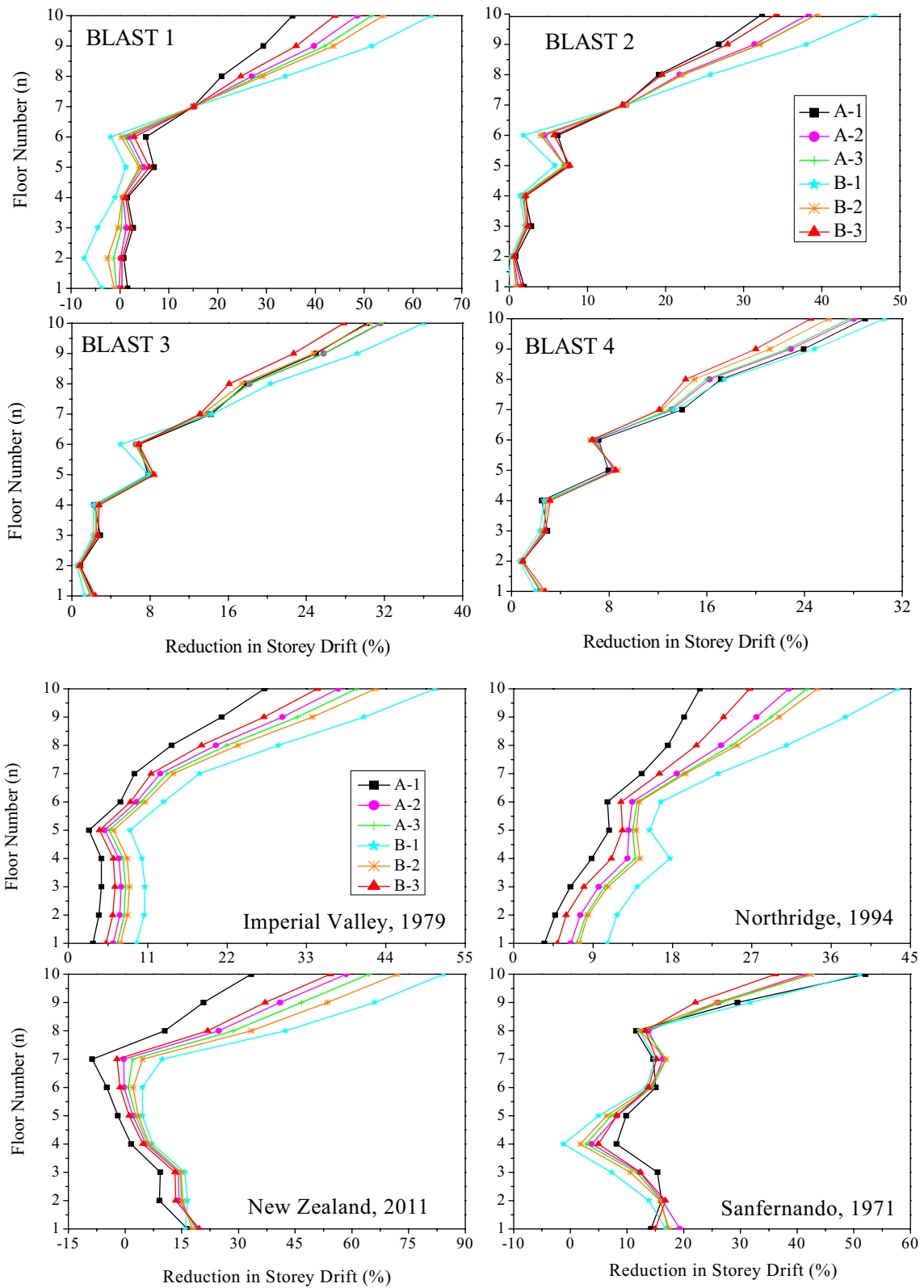
Fig. 14 Reduction in storey drift (%) under dynamic excitations due to placement of dampers (regular buildings)

Table 7 Structural performance of regular buildings under dynamic excitations [Damper-A]

Ground excitation	Damper A-1		Damper A-2		Damper A-3	
	Reduced maximum base shear (%)	Reduced maximum bending moment (%)	Reduced maximum base shear (%)	Reduced maximum bending moment (%)	Reduced maximum base shear (%)	Reduced maximum bending moment (%)
Blast 1	− 0.32	2.20	− 0.64	0.06	− 0.74	− 0.47
Blast 2	− 0.29	2.67	− 0.56	1.73	− 0.60	1.53
Blast 3	− 0.28	3.0	− 0.52	2.74	− 0.517	2.70
Blast 4	− 0.275	3.17	− 0.45	3.24	− 0.453	3.26
Imperial Valley	1.47	3.21	4.03	5.97	4.55	6.53
Northridge	1.02	3.22	4.17	6.24	4.94	6.91
New Zealand	17.74	18.88	18.02	20.0	17.63	19.36
San Fernando	8.43	13.63	11.70	15.90	12.11	16.51

Table 8 Structural performance of regular buildings under dynamic excitations [Damper-B]

Ground excitation	Damper A-1		Damper A-2		Damper A-3	
	Reduced maximum base shear (%)	Reduced maximum bending moment (%)	Reduced maximum base shear (%)	Reduced maximum bending moment (%)	Reduced maximum base shear (%)	Reduced maximum bending moment (%)
Blast 1	− 0.84	− 2.90	− 0.79	− 0.99	− 0.61	0.83
Blast 2	− 0.77	0.20	− 0.66	1.47	− 0.52	2.36
Blast 3	− 0.66	1.97	− 0.60	2.83	− 0.44	3.26
Blast 4	− 0.63	2.78	− 0.51	3.47	− 0.39	3.72
Imperial Valley	7.0	9.18	4.89	6.94	3.08	4.98
Northridge	8.34	10.43	5.53	7.25	2.93	4.76
New Zealand	16.21	16.61	16.85	18.48	18.0	20.52
San Fernando	13.84	17.03	12.02	16.71	10.35	14.39

Table 9 Structural performance of irregular buildings under dynamic excitations [Damper-A]

Ground excitation	Damper A-1		Damper A-2		Damper A-3	
	Reduced maximum base shear (%)	Reduced maximum bending moment (%)	Reduced maximum base shear (%)	Reduced maximum bending moment (%)	Reduced maximum base shear (%)	Reduced maximum bending moment (%)
Blast 1	− 0.269	− 0.218	− 0.48	− 0.29	− 0.51	− 0.294
Blast 2	16.70	8.0	16.73	8.02	16.75	8.02
Blast 3	− 0.21	− 0.19	− 0.405	− 0.27	− 0.405	− 0.28
Blast 4	16.69	8.0	16.76	8.0	16.76	8.01
Imperial Valley	14.10	10.73	18.18	15.20	18.96	16.08
Northridge	29.93	28.56	34.02	32.87	34.87	33.66
New Zealand	20.20	26.47	22.83	29.80	23.26	30.34
San Fernando	14.16	28.01	19.37	25.86	18.25	25.36

Table 10 Structural performance of irregular buildings under dynamic excitations [Damper-B]

Ground excitation	Damper B-1		Damper B-2		Damper B-3	
	Reduced maximum base shear (%)	Reduced maximum bending moment (%)	Reduced maximum base shear (%)	Reduced maximum bending moment (%)	Reduced maximum base shear (%)	Reduced maximum bending moment (%)
Blast 1	− 0.574	− 0.285	− 0.54	− 0.29	− 0.48	− 0.29
Blast 2	16.76	8.03	16.77	8.03	16.73	8.01
Blast 3	− 0.50	− 0.291	− 0.50	− 0.287	− 0.40	− 0.26
Blast 4	16.76	8.02	16.76	8.01	16.70	8.0
Imperial Valley	22.14	20.14	19.65	16.62	16.77	13.28
Northridge	37.65	36.04	35.25	34.16	32.21	30.92
New Zealand	23.12	28.54	22.76	30.94	22.19	29.03
San Fernando	12.39	23.04	17.18	24.87	19.56	26.36

isolation period (T_b) equals 1.5, 2.0 and 3 T_s (where T_s is structure period) to improve the structural performance. The study has been further extended to evaluate the performance of buildings equipped with fluid viscous dampers developed by M/s Taylor Devices, USA. The vital conclusions observed from the analysis of buildings equipped with isolation systems and viscous dampers are as follows:

1. The selected isolation systems are effective in reducing the floor acceleration response and storey drift in the buildings subjected to blast and earthquake excitations. It is observed that the base isolation systems perform better in buildings plagued with irregularity as compared to regular base-isolated buildings. The study reveals that an isolation system with $T_b = 3$ T_s results in maximum reductions in damage indices, such as top storey displacement, acceleration, bottom column forces and upholds the assumptions proposed by the seismic design handbook [16].

2. It is also observed that an isolation system with $T_b = 3$ T_s results in the maximum bearing displacement with least value of shear force, hereby leading to the maximum energy dissipated by the system. Moreover, an increase in the isolation period reduces the energy dissipated along with input energy for seismic conditions thus resulting in maximum percentage of energy dissipated under earthquake and blast excitations.

3. It is also observed that the selected FVDs also show significant reductions in structural damage indices under blast and seismic loading for regular and irregular buildings. However, the ability to mitigate bottom column responses is marginal for blast-induced vibrations when compared with seismic tremors.

4. The FVDs with least damping exponent and appreciable damping coefficient, i.e., Damper B-1 outperforms other selected dampers with high damping exponent and damping coefficient in mitigating the structural responses.

5. The force deformation behavior of Damper B-1 undergoes maximum axial force along with appreciable deformations resulting in maximum energy dissipated for all cases of selected ground vibrations and thus resulting in maximum reductions in structural responses.

6. It can finally be concluded that both FVDs and base isolation system perform effectively under selected dynamic loading with FVDs proving to be an excellent alternative to base isolation technique subjected to blast and seismic vibrations.
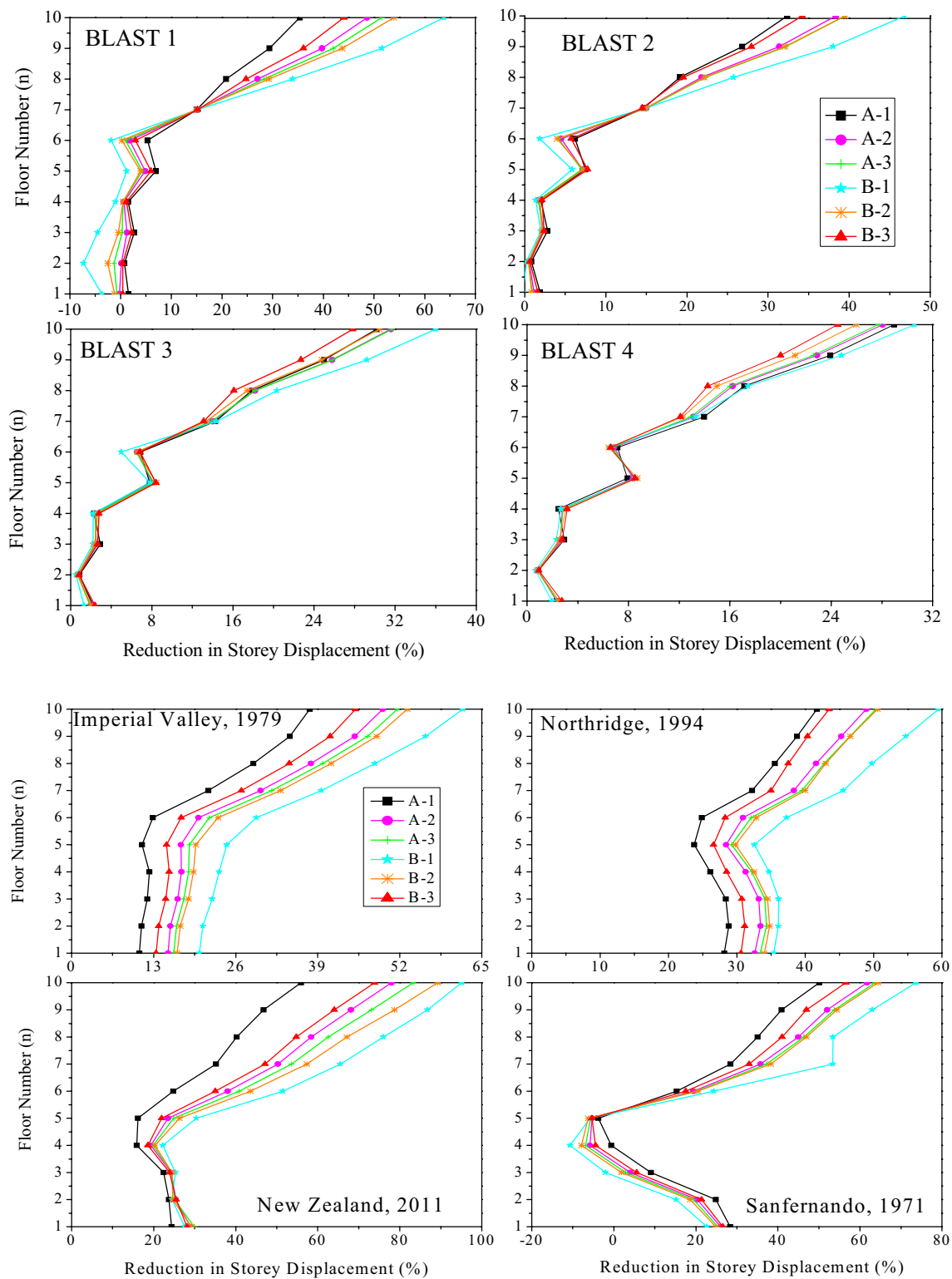
Fig. 15 Reduction in Storey Drift (%) under dynamic excitations due to placement of dampers (irregular buildings)
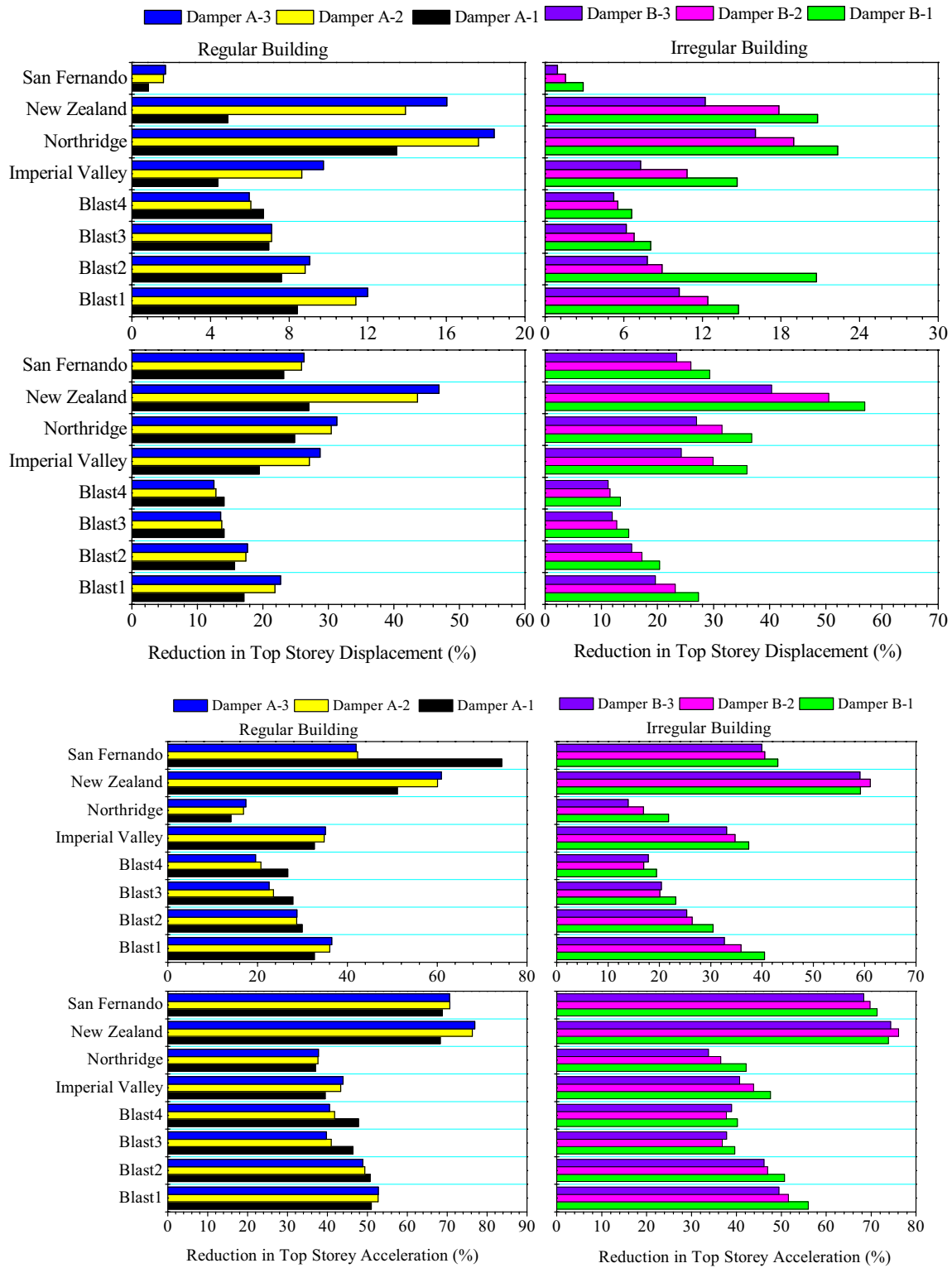
Fig. 16 Performance of steel buildings equipped with viscous dampers under dynamic loading
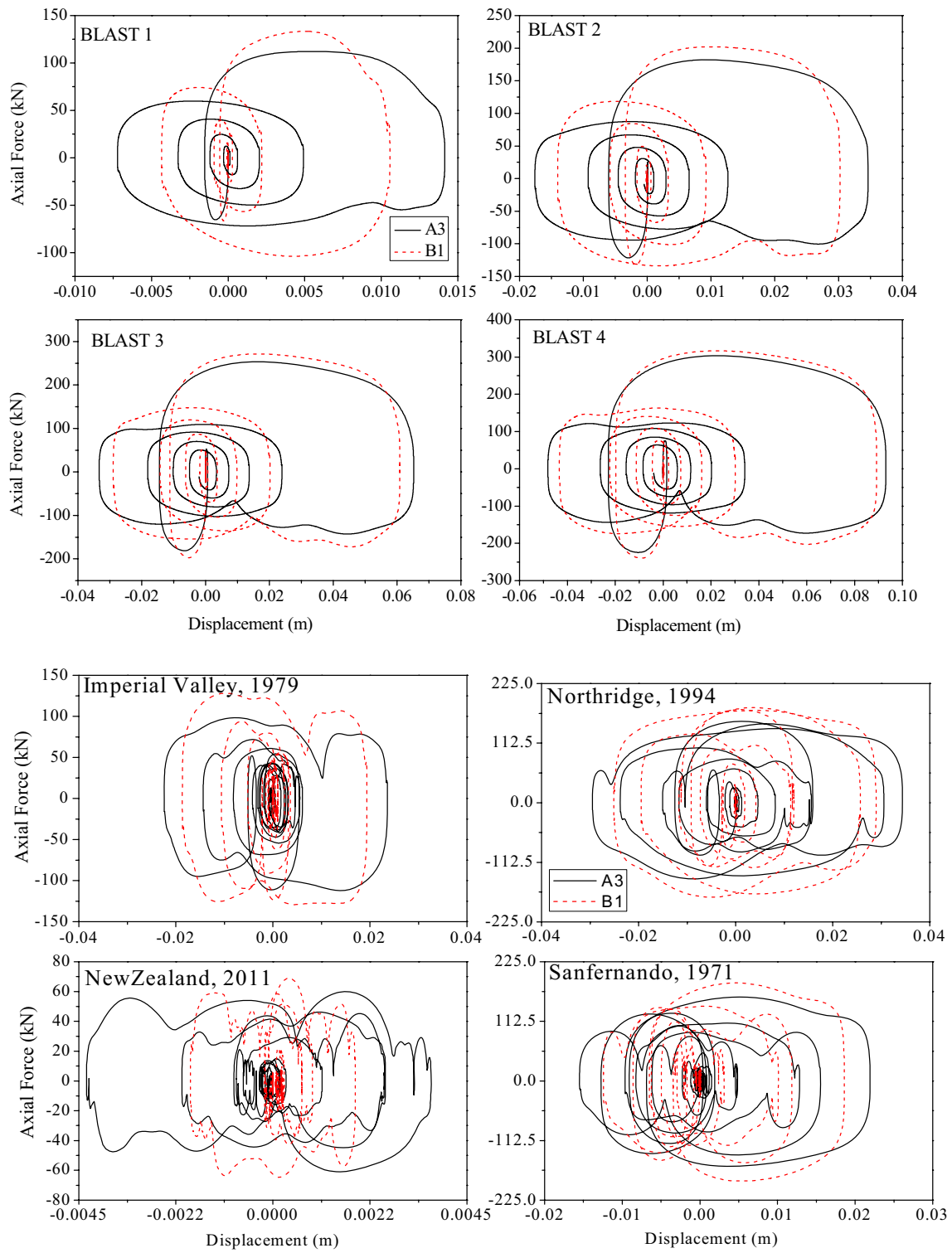
Fig. 17 Force displacement behavior of dampers A-3 and B-1 under selected ground excitations (regular building)
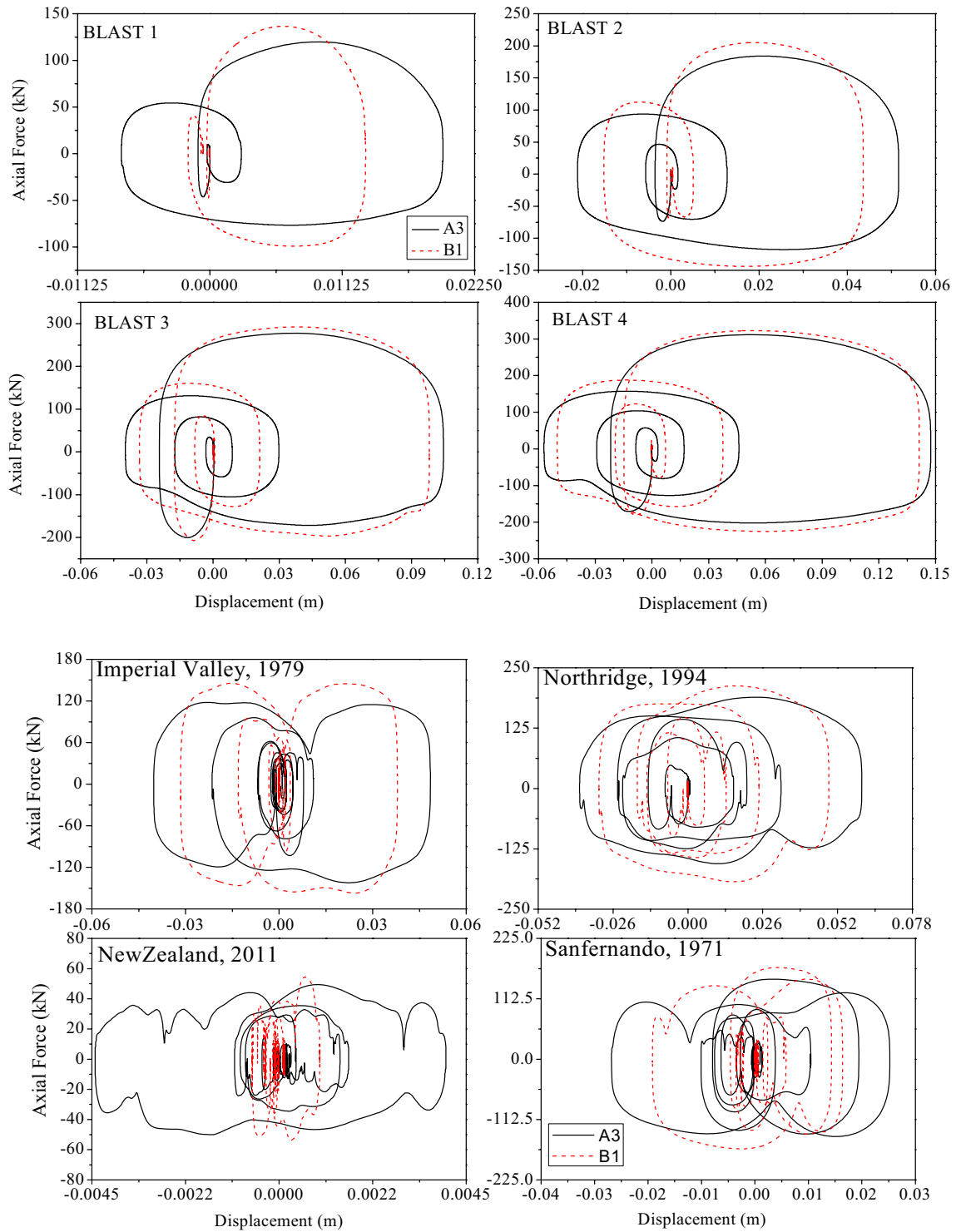
Fig.18 Force displacement behavior of dampers A-3 and B-1 under selected ground excitations (irregular building)
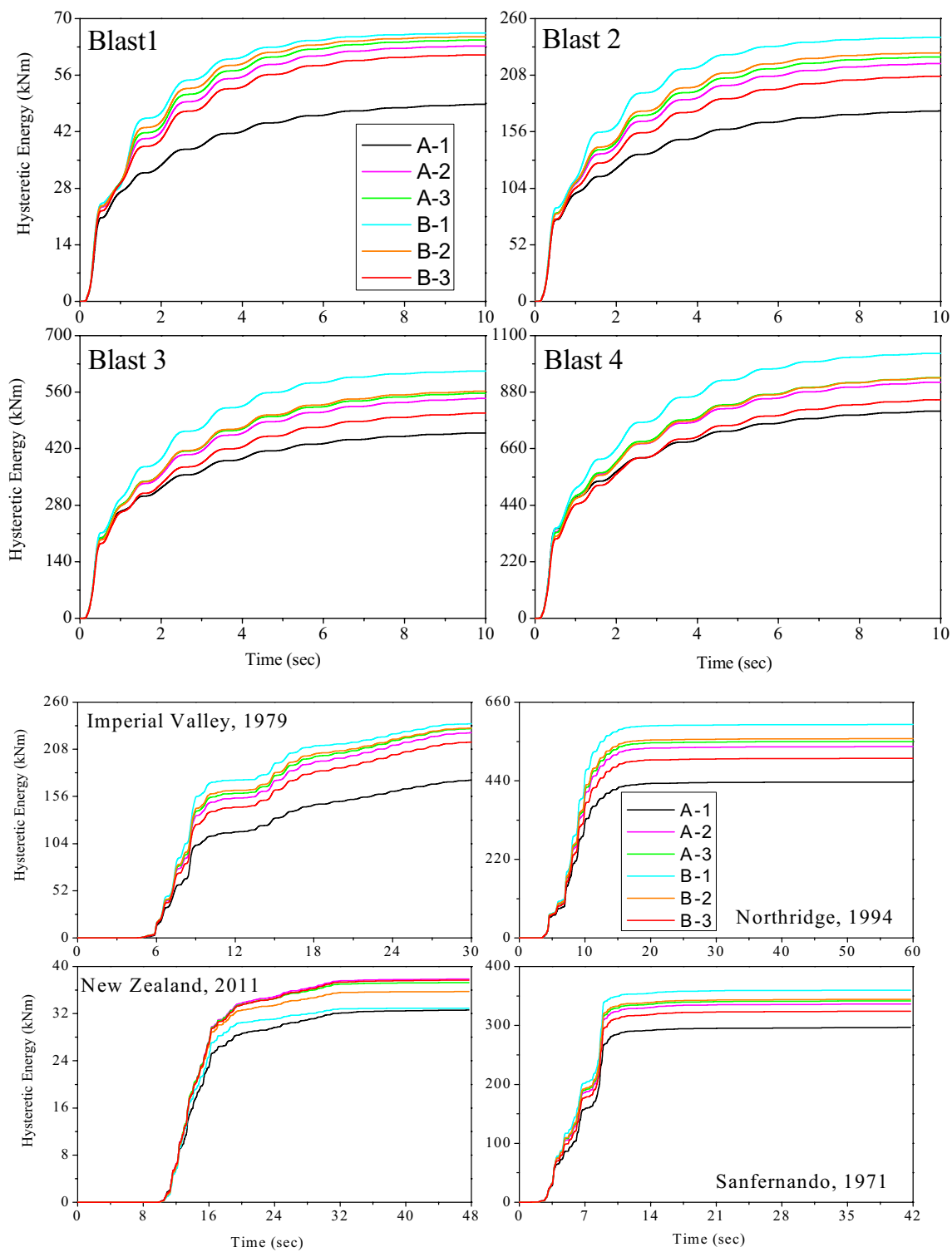
Fig. 19 Energy dissipated by selected dampers in mitigating structural responses under selected excitations (regular building)
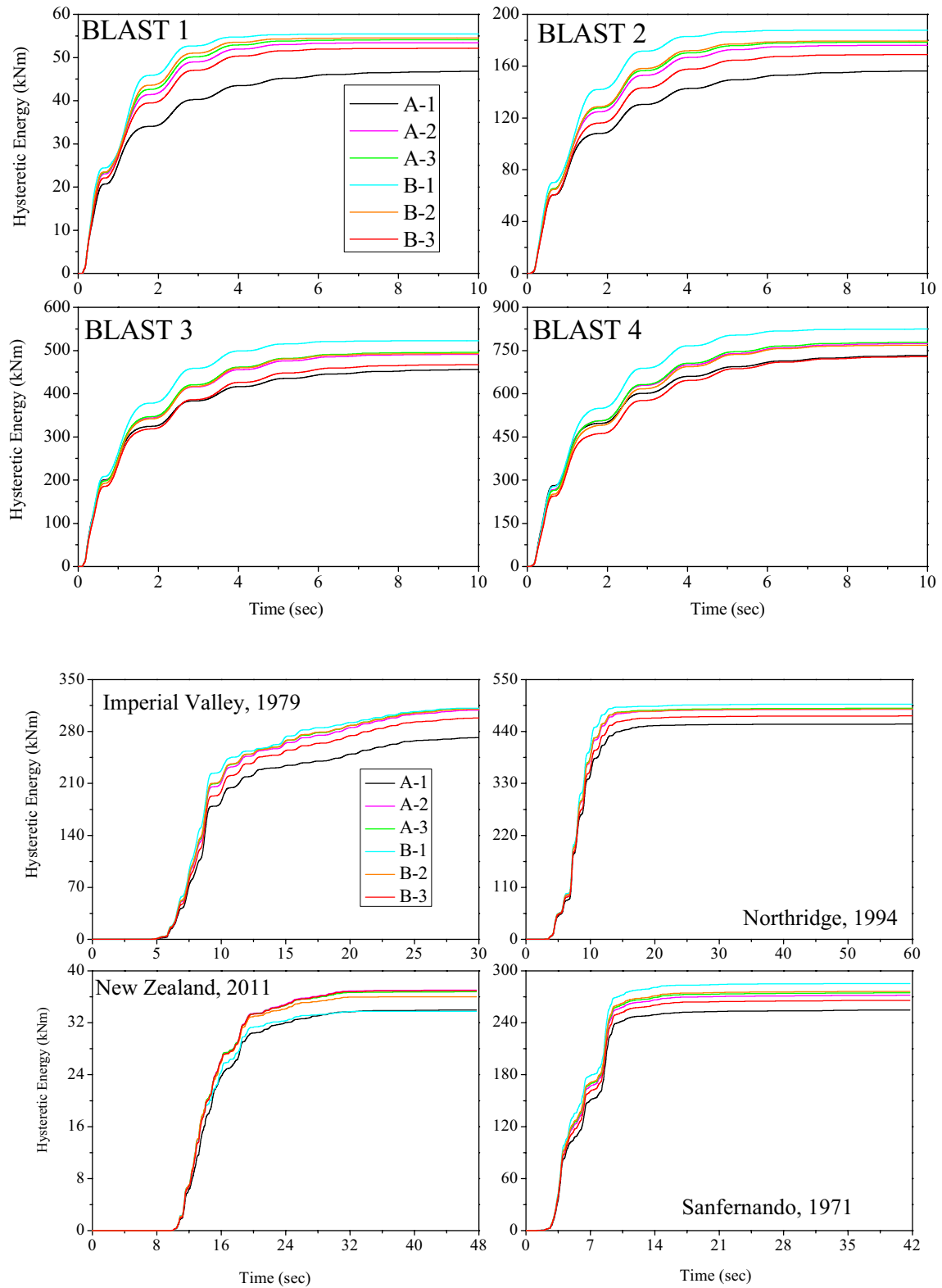
Fig. 20 Energy dissipated by selected dampers in mitigating structural responses under selected excitations (irregular building)

Table 11 Percentage of energy dissipated by the passive systems installed in regular building

Passive system	Blast 1	Blast 2	Blast 3	Blast 4	Imperial Valley	Northridge	New Zealand	San Fernando
Damper A-1	32.76	30.77	29.27	28.4	27.03	27.02	37.03	44.69
Damper A-2	42.46	38.42	34.69	32.36	36.52	33.82	43.33	48.38
Damper A-3	43.45	39.5	35.53	32.98	37.65	34.92	43	48.7
Damper B-1	44.61	42.66	39.03	36.31	40.32	38.94	39.3	49.36
Damper B-2	44	40.18	35.83	32.94	38.28	35.55	41.84	48.68
Damper B-3	40.98	36.39	32.38	29.96	34.6	31.46	42.95	47.27
LRB ($T_b = 1.5\ T_s$)	63.5	60.72	52.7	46	51.32	56.29	49.67	32.4
LRB ($T_b = 2.0\ T_s$)	70.6	66.15	56.96	48.9	58.98	62.56	57	38.39
LRB ($T_b = 3.0\ T_s$)	76.59	68.83	55.96	46.21	64.29	67.3	69.43	45.06

Table 12 Percentage of energy dissipated by the passive systems installed in irregular building

Passive system	Blast 1	Blast 2	Blast 3	Blast 4	Imperial Valley	Northridge	New Zealand	San Fernando
Damper A-1	55.90	49.40	51.73	46.43	50.36	50.86	56.16	61.97
Damper A-2	63.82	55.62	55.70	49.04	59.13	57.53	61.56	64.84
Damper A-3	64.66	56.42	56.20	49.32	60.33	58.47	61.32	65.11
Damper B-1	66.29	59.35	59.30	52.22	64.29	62.22	58.06	65.82
Damper B-2	65.17	56.70	55.92	48.69	60.97	58.77	60.46	65.10
Damper B-3	62.29	53.40	53.0	46.15	56.46	54.68	61.21	63.83
LRB ($T_b = 1.5\ T_s$)	62.86	59.15	50.41	44.24	54.35	54.33	44.44	32.42
LRB ($T_b = 2.0\ T_s$)	70.97	65.04	55.17	48.55	60.84	58.30	57.21	39.60
LRB ($T_b = 3.0\ T_s$)	77.85	69.0	57.91	51.77	65.24	61.47	65.66	46.94

References

1. BIS (Bureau of Indian Standards) (1973) IS 6922: Indian Standard criteria for safety and design of structures subject to underground blast, New Delhi, India
2. BIS (Bureau of Indian Standards) (1968) IS 4991: Indian standard criteria for blast resistant design of structures for explosions above ground, New Delhi, India
3. UFC 3-340-02 (2008) Department of Defense-Structures to resist the effects of accidental explosions, Washington, DC, United States of America
4. FEMA 428 (Federal Emergency Management Agency) (2003) Primer to Design Safe School Projects in Case of Terrorist Attacks, United States of America
5. NATO AC/258-D/258 (1993) Manual of NATO safety principles for the storage of NATO ammunition and explosives, Bonn, Germany
6. Kumar R, Choudhury D, Bhargava K (2013) Prediction of blast-induced vibration parameters for soil sites. Int J Geomech. https://doi.org/10.1061/(ASCE)GM.1943-5622.0000355
7. Rigas F, Ioannis S (1999) Amplification effects of soil stratification on ground stress waves. J Geotech Geoenviron Eng 125(7):611–614
8. Wu C, Lu Y, Hao H, Lim WK, Zhou Y, Seah CC (2003) Characterisation of underground blast-induced ground motions from large-scale field tests. Shock Waves 13(3):237–252
9. Wu C, Hao H (2005) Numerical study of characteristics of underground blast induced surface ground motion and their effect on above-ground structures. Part I. Ground motion characteristics. Soil Dyn Earthq Eng 25(1):27–38
10. Mondal PD, Ghosh AD, Chakraborty S (2017) Performances of various base isolation systems in mitigation of structural vibration due to underground blast induced ground motion. Int J Struct Stab Dyn 17(4):1750043
11. Wu C, Hao H, Lu Y, Sun S (2004) Numerical simulation of structural responses on a sand layer to blast induced ground excitations. Comput Struct 82(9):799–814
12. Mondal PD, Ghosh A, Chakraborty S (2014) Control of underground blast induced vibration of structures using fluid viscous damper. J Vib Eng Technol 2(1):27–33
13. Soong TT, Dargush GF (1997) Passive energy dissipation systems in structural engineering. Wiley, Chichester, pp 1–180
14. Su L, Ahmadi G, Tadjbakhsh IG (1989) A comparative study of performances of various base isolation systems, part I: shear beam structures. Earthq Eng Struct Dyn 18(1):11–32
15. Jangid RS (1996) Seismic response of sliding structures to bidirectional earthquake excitation. Earthq Eng Struct Dyn 25(11):1301–1306
16. Naeim F (2001) The seismic design handbook, 2nd edn. Springer, New York, pp 724–745
17. Necdet T (2004) Seismic isolation and energy dissipating systems in earthquake resistant design. In: Proc. 13th World conference on earthquake engineering, 13WCEE, Vancouver, Canada
18. Rodrigo MM, Romero ML (2003) An optimum retrofit strategy for moment resisting frames with nonlinear viscous dampers for seismic applications. Eng Struct 25(7):913–925
19. Constantinou MC, Tadjbakhsh IG (1985) Hysteretic dampers in base isolation: random approach. J Struct Eng 111(4):705–721
20. Kelly JM, Leitmann G, Soldatos AG (1987) Robust control of base-isolated structures under earthquake excitation. J Optim Theory Appl 53(2):159–180

21. Johnson EA, Ramallo JC, Spencer Jr BF, Sain MK (2002) Intelligent base isolation systems. Second World Conference on Structural Control, Kyoto, Japan
22. Jangid RS, Kelly JM (2001) Base isolation for near-fault motions. Earthq Eng Struct Dyn 30(5):691–707
23. Housner GW, Bergman LA, Caughey TK, Chassiakos AG, Claus RO, Masri SF, Skelton RE, Soong TT, Spencer BF, Yao JT (1997) Structural control: past, present, and future. J Eng Mech 123(9):897–971
24. Lin YY, Tsai MH, Hwang JS, Chang KC (2002) Direct Displacement based design for building with passive energy dissipation systems. Eng Struct 25(1):25–37
25. Kokil AS, Shrikhande M (2007) Optimal placement of supplemental dampers in seismic design of structures. J Seismol Earthq Eng 9(3):125–135
26. Singh MP, Moreschi LM (2002) Optimal placement of dampers for passive response control. Earthq Eng Struct Dyn 31(4):955–976
27. Dargush GF, Sant RS (2005) Evolutionary aseismic design and retrofit of structures with passive energy dissipation. Earthq Eng Struct Dyn 34(13):1601–1626
28. Park JH, Kim J, Min KW (2004) Optimal design of added visco elastic dampers and supporting braces. Earthq Eng Struct Dyn 33(4):465–484
29. Di Sarno L, Chioccarelli E, Cosenza E (2011) Seismic response analysis of an irregular base isolated building. Bull Earthq Eng 9(5):1673–1702
30. Cancellara D, Angelis FD (2017) Assessment and dynamic nonlinear analysis of different base isolation systems for a multi-storey RC building irregular in plan. Comput Struct 180:74–88
31. Goel RK (2004) Seismic response control of irregular structures using nonlinear dampers. In: Proceedings of the 13th world conference on earthquake engineering
32. Hinman EE (1989) Shock response of buried structures subject blast. Proc., ASCE Spec. Conf. on Structures for Enhanced Safety and Physical Security, 191–202
33. Carvalho EM, Battista RC (2003) Blast-induced vibrations in urban residential buildings. Proc Inst Civ Eng Struct Build 156(3):243–253
34. Kumar R, Choudhury D, Bhargava K (2016) Determination of blast-induced ground vibration equations for rocks using mechanical and geological properties. J Rock Mech Geotech Eng 8(3):341–349
35. CSI (Computers and Structures Inc.) (2004) SAP2000 v10 Integrated Finite Element Analysis and Design of Structures.CSI, Berkeley
36. Whittle JK, Williams MS, Karavasilis TL, Blakeborough A (2012) A comparison of viscous damper placement methods for improving seismic building design. J Earthq Eng 16(4):540–560
37. BS (British Standard) (2004) EN-1998-1- Eurocode 8: design of structures for earthquake resistance-part 1: general rules, seismic actions and rules for buildings
38. BIS (Bureau of Indian Standards) (2016) IS 1893 (Part 1)-Indian standard criteria for earthquake resistant design of structures, Part 1—general provisions and buildings, New Delhi
39. UBC (Uniform building code) (1997) International conference of building officials (ICBO), Whittier, California
40. Uang CM, Bertero VV (1990) Evaluation of seismic energy in structures. Earthq Eng Struct Dyn 19(1):77–90
41. Haskell G, Lee D (1996) Fluid viscous damping as an alternative to base isolation. Asme Publ Pvp 330:35–40
42. Ras A, Boumechra N (2014) Study of nonlinear fluid viscous dampers behaviour in seismic steel structures design. Arab J Sci Eng 39(12):8635–8648
43. Narkhede DI, Sinha R (2014) Behavior of nonlinear fluid viscous dampers for control of shock vibrations. J Sound Vib 333(1):80–98